Chemical Papers
https://doi.org/10.1007/s11696-019-00918-3

ORIGINAL PAPER

Synthesis and characterization of one impurity in esomeprazole, an antiulcerative drug

Zhen-Tao Liu[1] · Xia Meng[1] · Shi-Min Fang[1] · Li-Zhen Wang[2] · Zhen-Zheng Wang[1] · Geng Yang[1] · Hong-Dong Duan[1] · Ai-You Hao[3]

Received: 18 January 2019 / Accepted: 28 August 2019

Abstract
During drug synthesis, control of impurities is very important to get high-qualified drugs. A number of studies have devoted to synthesize the impurities and study the structures to support the method of purification. In this paper, we first synthesize one impurity in esomeprazole, rel-2-[[(3,5-dimethyl-2-pyridinyl)methyl]sulfinyl]-6-methoxy-1*H*-benzimidazole, with readily available raw materials, simple operation procedures and relatively mild reaction. Besides, we characterized its structure by MS, IR, ^{1}H-NMR and HPLC analyses. The purity of target compound is as high as 99.58%, which can be used as the reference substance of the impurities of esomeprazole.

Keywords Characterization · Esomeprazole · Impurity · Synthesis

Introduction

Esomeprazole, the *S*-isomer of omeprazole (Vakil et al. 2001), is the first single optical isomer proton pump inhibitor in the clinics (Thitiphuree and Talley 2000). Esomeprazole is a weak alkaline wall cell proton pump H/K-ATP enzyme-specific and non-competitive inhibitor (Andersson et al. 2001), which acts on gastric parietal cells to prevent gastric acid formation and reduce gastric acid secretion by inhibiting H/K- activity (Tonini et al. 2001). At present, esomeprazole is widely used to treat gastro-oesophageal reflux diseases (Sugimoto and Furuta 2012) and other acid-related diseases (Tang and Wu 2013), due to its strong acid inhibition, high specificity and long duration (Cardile and Romano 2012). Additionally, esomeprazole can cure peptic ulcer rapidly by inhibiting the secretion of gastric acid (Sugano et al., 2012) and effectively scavenging *Helicobacter pylori* (Cheng et al. 2014).

Because of the limitation of production technology, some impurities are extremely difficult to be completely removed (Manimaran and Stahly 1993), which will affect the stability and efficacy of the drug or even hurt the health without therapeutic effects (Stawny et al. 2016). As for esomeprazole, always containing many impurities, the control requirements for impurities are very strict (Reddy 2013). Of note, we are interested in one specific impurity, 5-methoxy-2-[(3,5-dimethylpyridin-2-yl)methylsulfinyl]-1*H*-benzimidazole (compound **1**), which has a similar chemical structure with esomeprazole and is hard to be removed thoroughly. Therefore, this article aimed at developing efficient synthesis process of this impurity, and laying a foundation for the detection and control of esomeprazole impurities. The main synthetic routes are as follows (Fig. 1).

Experimental

All reagents and solvents were purchased from common commercial suppliers and were used without further purification. The melting point was measured by micro-melting point meter WRS-2. The IR spectra were recorded on a

Electronic supplementary material The online version of this article (https://doi.org/10.1007/s11696-019-00918-3) contains supplementary material, which is available to authorized users.

✉ Hong-Dong Duan
hdduan67@163.com

[1] School of Chemistry and Pharmaceutical Engineering, Qilu University of Technology (Shandong Academy of Sciences), Jinan 250353, China

[2] Biology Institute, Qilu University of Technology (Shandong Academy of Sciences), Jinan 250014, China

[3] School of Chemistry and Chemical Engineering, Shandong University, Jinan 250012, China

Published online: 03 September 2019

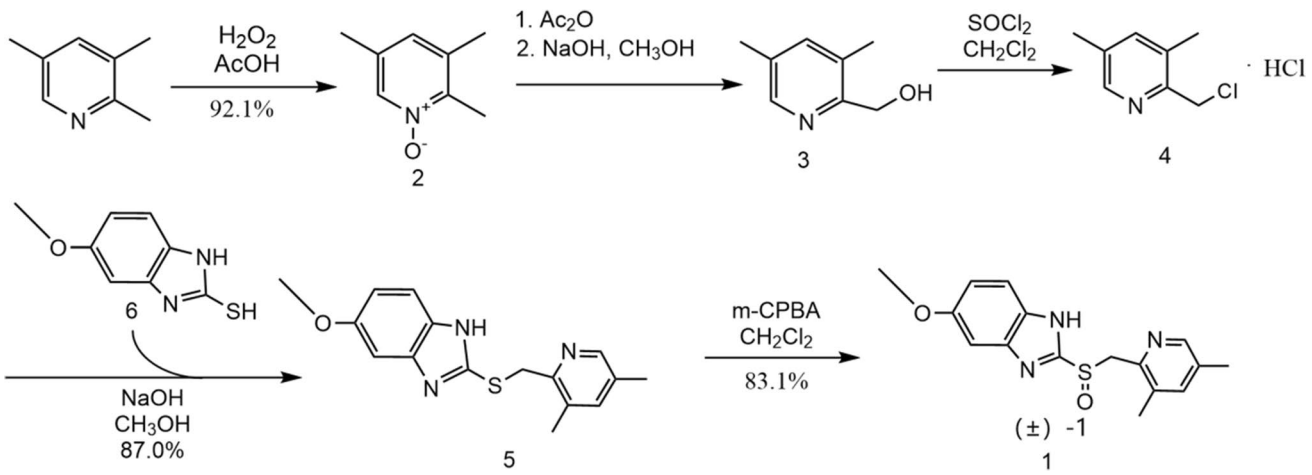

Fig. 1 The synthetic route of compound **1**

TENSOR-IR spectrometer. The NMR spectra were recorded in $CDCl_3$ solution or DMSO solution on an AVANCE II 400 MHz. Agilent 1260 was used to determine product purity. High-resolution mass spectrometry is obtained by MTQ III q-TOF.

Synthesis of 5-methoxy-2-[(3,5-dimethylpyridin-2-yl) methylsulfinyl]-1*H*-benzimidazole (compound 1)

2,3,5-Trimethylpyridine (6.06 g, 0.050 mol) was added into acetic acid solution (14.0 mL), and the mixture was stirred and mixed evenly, heated to 98–100 ℃. Then hydrogen peroxide (9.70 g, 30%) was slowly dropped into the solution, after which, the reaction mixture was heated and refluxed for 1.0 h, and the reaction progress was detected by TLC (ethyl acetate as unfolding agent). After the reaction, the reaction solution was concentrated. The mixture was evaporated under reduced pressure to remove acetic acid until no liquid is vaporized. Subsequently, H_2O (10.0 mL) and dichloromethane (15.0 mL) were added to concentrated solution and then the pH of the solution was adjusted to 9.0 with sodium hydroxide solution. The water layer was extracted with dichloromethane (2 × 25.0 mL); the organic layers were combined and dried over anhydrous magnesium sulfate, filtered, and concentrated in vacuo to afford 2,3,5-trimethylpyridine-*N*-oxide (compound 2) as a white solid at 81% yield (5.58 g). m.p.: 42.4–43.8 ℃, IR (KBr): 3949.1, 2831.5, 1625.9, 949.0 (Fig. 2), ^{1}H NMR (400 MHz, $CDCl_3$) δ 8.02 (s, 1H), 6.88 (s, 1H), 2.47 (s, 3H), 2.29 (s, 3H), 2.23 (s, 3H) (Fig. 3). [^{1}H NMR (400 MHz, $CDCl_3$): d = 8.21 (s, H), 7.16 (s, H), 2.53 (s, 3H), 2.38 (s, 3H), 2.32 (s, 3H)] (Getter et al. 2015).

Compound **2** (1.37 g, 0.010 mol) was added to acetic anhydride (12.0 mL); the mixture was heated

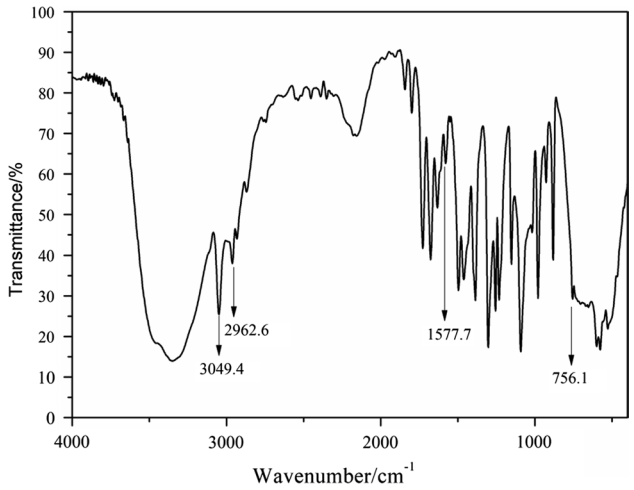

Fig. 2 FT-IR of compound **2**

to 70.0–75.0℃. TLC (unfolding agent—ethyl acetate:ethanol = 2:1) was used to detect the completion of the reaction. After the reaction, the reaction solution was concentrated. Then the product was dissolved with methanol (35.0 mL), and the sodium hydroxide (20.0 ml, 2.20 g of sodium hydroxide) solution was added to the solution. The reaction mixture was refluxed. TLC (unfolding agent—ethyl acetate:ethanol = 2:1) was used to detect the completion of the reaction. After the TLC detection reaction is completed and concentrated, dichloromethane is added to separate the liquid. The organic layers were combined and dried over anhydrous magnesium sulfate, filtered, concentrated in vacuum to afford 3,5-dimethyl-2-hydroxymethylpyridine (compound **3**) as a yellow sticky liquid. IR(KBr): 3394.7, 2922.1, 1573.9 (Fig. 4), ^{1}H NMR (400 MHz, $CDCl_3$) δ 8.22 (s, 1H), 7.29 (s, 1H), 4.65 (s, 2H), 2.31 (s, 3H), 2.18 (s, 3H) (Fig. 5). [^{1}H NMR

Fig. 3 ^{1}H NMR of compound **2**

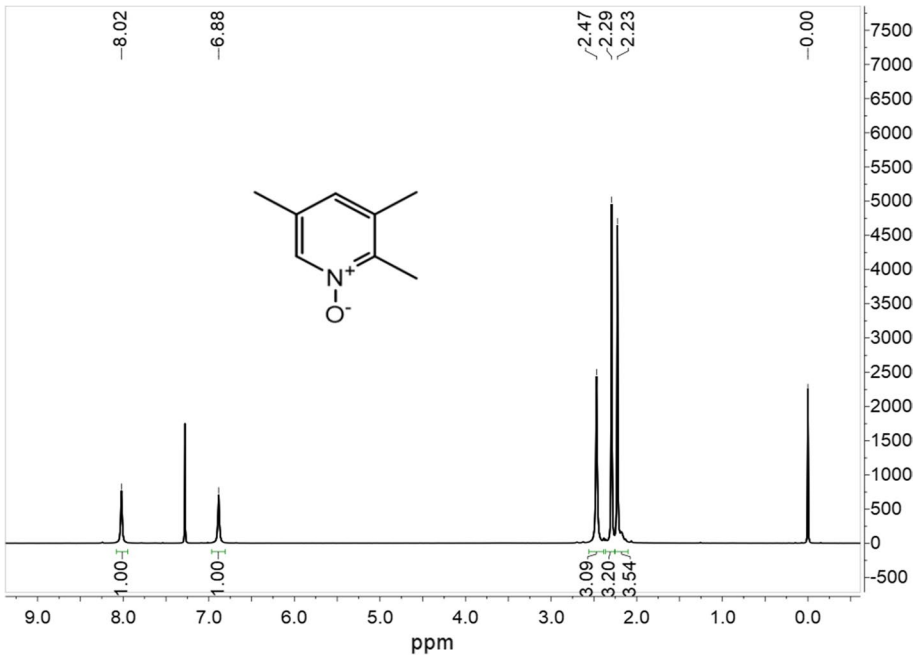

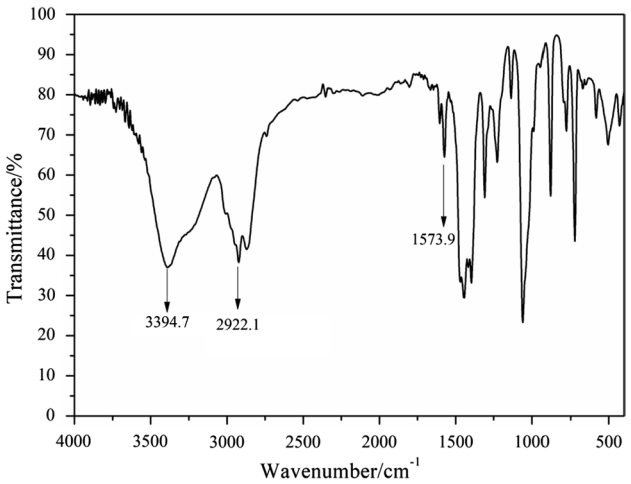

Fig. 4 FT-IR of compound **3**

(400 MHz,$CDCl_3$): $d = 8.12$ (s, H), 7.20 (s, H), 4.57 (s, 2H), 2.22 (s, 3H), 2.11 (s, 3H)] (Getter et al. 2015).

Compound **3** from the previous step was diluted by dichloromethane (20.0 mL), the solution was cooled to −5 to 0 ℃. Then $SOCl_2$ (4.0 mL) which was diluted by dichloromethane was dropped into the mixture solution. After the drop was finished, the reaction is held for 1 h and quenched by isopropanol. The dichloromethane was removed by the rotary evaporator until no liquid is distilled out, and the residual liquid turned into brown sticky grease. Then the acetonitrile was used to remove the liquid again by a rotary evaporator, and finally the yellow solid was obtained. The resulting residue was recrystallized in toluene to afford 2-chloromethyl-3,5-dimethylpyridine hydrochloride (compound **4**) as a yellow solid at 45% overall yield (0.70 g). m.p.: 106.0–106.6℃, IR (KBr): 2996.2, 1621.5, 675.1 (Fig. 6), ^{1}H NMR (400 MHz, $CDCl_3$) δ 8.40 (s, 1H), 8.02 (s, 1H), 5.15 (s, 2H), 2.62 (s, 3H), 2.55 (s, 3H) (Fig. 7). ^{13}C NMR (101 MHz, DMSO) δ 147.75 (s), 146.86 (s), 140.05 (s), 137.81 (s), 136.88 (s), 17.95 (s), 17.15 (s) (Fig. 8). m/z $[M+H]^+$ calcd for: $C_8H_{10}ClN$: 156.0580, found: 156.0581 (Fig. 9).

Compound **4** (2.88 g, 0.015 mol) and 2-mercapto-5-methoxy benzimidazole (2.70 g, 0.015 mol) were dissolved in methanol solution (18.0 mL), then the sodium hydroxide solution (10.00 g, 2.50 g of sodium hydroxide) was dropped to mixture, and the reaction mixture was heated to 55.0–60.0 ℃. Detection of reaction progress by TLC (unfolding agent—dichloromethane:ethyl acetate = 2:1). After the reaction is completed, the white solid impurities are removed by filtration. Concentrate the filtrate until no liquid is removed. Then dichloromethane (15.0 mL) and H_2O (15.0 mL) were added, the pH value was adjusted to 7 with acetic acid (15%). The mixture was stirred for 10 min and then extracted with dichloromethane and water. The dichloromethane (25.0 mL) was added to the aqueous phase, and the organic phase was merged after two extractions, the organic layers were dried over anhydrous magnesium sulfate, filtered, concentrated in vacuum to afford 2-[(3, 5-dimethyl-2-pyridinyl) methylthio)]-5-methoxy-1*H*-benzimidazole (compound **5**) as a white solid (3.90 g, yield 87%): m.p.: 53.7–59.5 ℃, IR (KBr): 3949.1, 2831.5, 1625.9, 949.0 (Fig. 10), ^{1}H NMR (400 MHz, DMSO) δ 12.48 (s, 1H), 8.20 (s, 1H), 7.43 (d, $J = 8.7$ Hz, 1H), 7.11 (d,

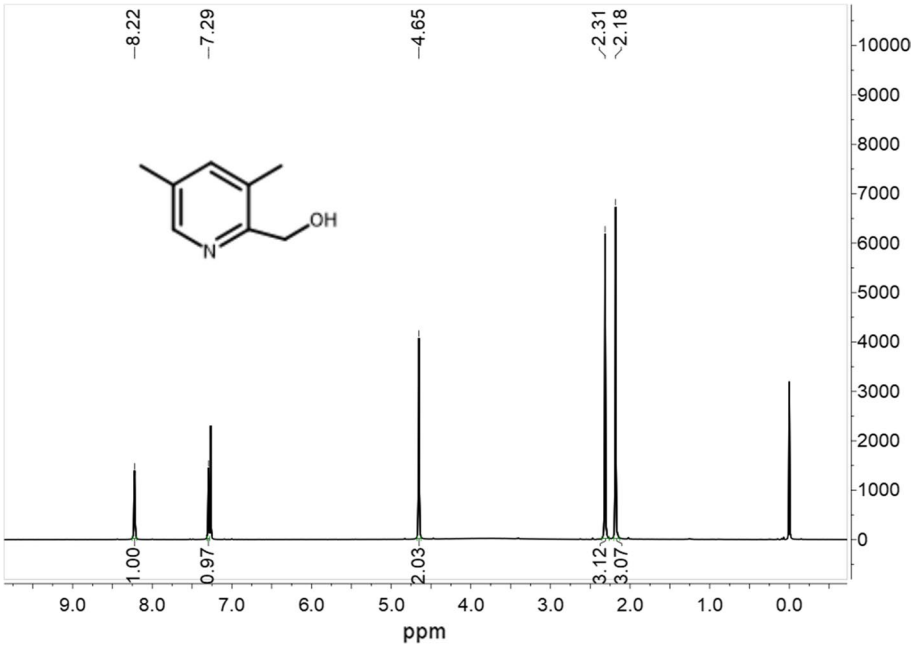

Fig. 5 ^{1}H NMR of compound **3**

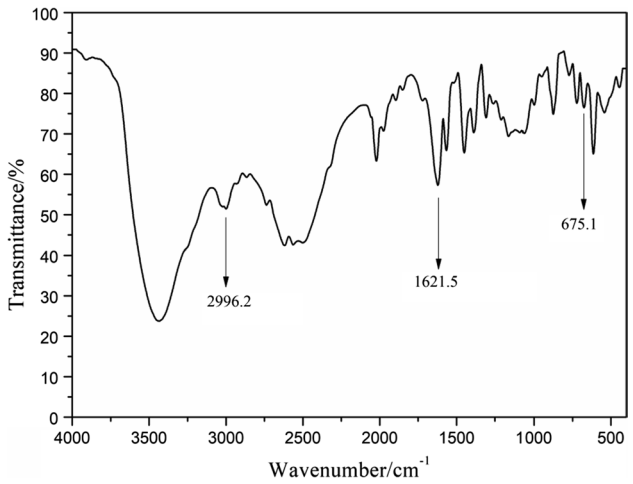

Fig. 6 FT-IR of compound **4**

J = 1.8 Hz, 1H), 6.92 (d, J = 2.1 Hz, 1H), 6.78 (t, J = 6.3 Hz, 1H), 4.68 (s, 1H), 4.65 (s, 1H), 3.80 (s, 3H), 2.38 (s, 3H), 2.28 (s, 3H) (Figure 11). ^{13}C NMR (101 MHz, DMSO) δ 151.89 (s), 147.09 (s), 139.01 (s), 132.46 (s), 131.51 (s), 56.52 (s), 55.91 (s), 36.59 (s), 18.36 (s), 17.86 (s) (Fig. 12), m/z $[M+H]^+$ calcd for: $C_{16}H_{17}N_3OS$: 300.1171, found: 300.1172 (Fig. 13).

3-Chloroperoxybenzoic acid, diluted by dichloromethane, was dropped into a mixture of dichloromethane (20.0 mL) and compound **5** (2.99 g, 0.010 mol) under low temperature (− 5 to 0 ℃). The reaction process was monitored by TLC (unfolding agent—dichloromethane:methyl tert butyl ether = 2:1). When the reaction is almost complete, stop dropping *m*-chloroperoxybenzoic acid. Peroxides in solution were detected with potassium iodide–starch test paper, and then 20.0 mL distilled water was added into the solution. Then the pH value of the solution was adjusted to 7 with potassium carbonate solution. The mixture was stirred for 10 min and then the liquid was separated. The dichloromethane layer was extracted with water (2 × 25.0 mL). Then the organic layers were combined with being dried over anhydrous magnesium sulfate and filtered. The dichloromethane in the filtrate is removed by a rotary evaporator. After 5–7 h at − 5 to 0 ℃, the crude product is recrystallized by methanol (5–8 mL) to get 2-(3,5-dimethyl-2-pyridinyl)methylsulfinyl-5-methoxy-1*H*-benzimidazole (compound **1**) as a white solid in (2.61 g, yield 83%): m.p.: 166.1–166.5 ℃, IR (KBr): 2989.6, 1625.9, 964.4 (Fig. 14), ^{1}H NMR (400 MHz, DMSO) δ 13.45 (s, 1H), 8.19 (s, 1H), 7.55 (d, J = 7.8 Hz, 1H), 7.45 (s, 1H), 7.09 (s, 1H), 6.96–6.86 (m, 1H), 4.75 (d, J = 12.0 Hz, 1H), 4.67 (d, J = 12.0 Hz, 1H), 3.81 (s, 3H), 2.28 (s, 3H), 2.25 (s, 3H) (Fig. 15), m/z $[M+H]^+$ calcd for: $C_{16}H_{17}N_3O_2S$: 316.1120, found: 316.1107 (Fig. 16). ^{13}C NMR (101 MHz, DMSO) δ 147.60 (s), 147.36 (s), 139.04 (s), 133.32 (s), 132.81 (s), 60.21 (s), 55.98 (s), 18.56 (s), 17.90 (s) (Fig. 17).

Results and discussion

The synthesis of compound **2** and **3** mainly refers to the work of Tamar Gatter et al. Compound **3** was synthesized using the Boekelheide rearrangement (Boekelheide and Linn 1954). And a modification of the procedure reported has been carried out as per Ellervik and Magnusson (2010). We made some modifications by their experiments.

Fig. 7 ^{1}H NMR of compound **4**

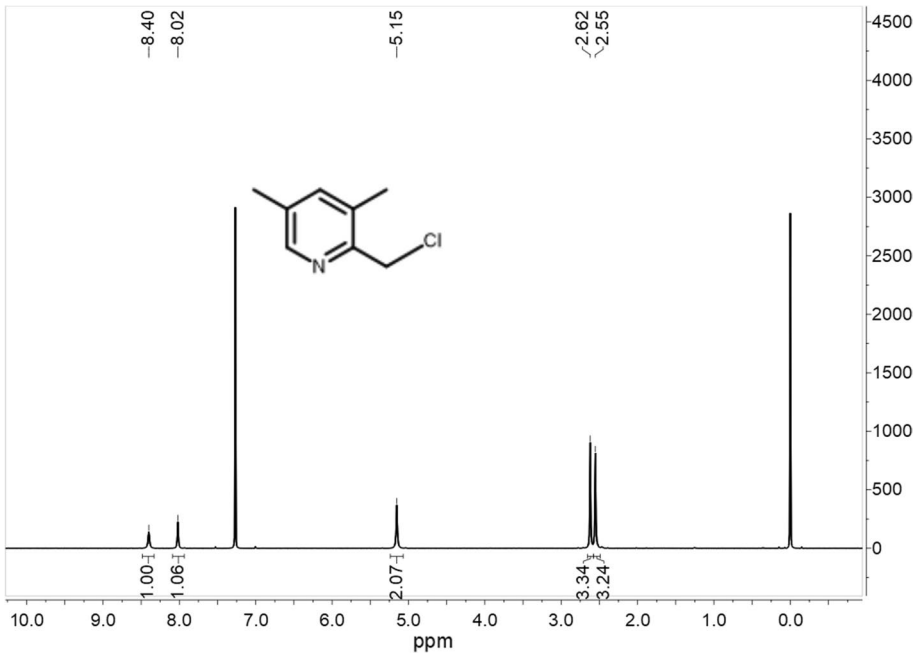

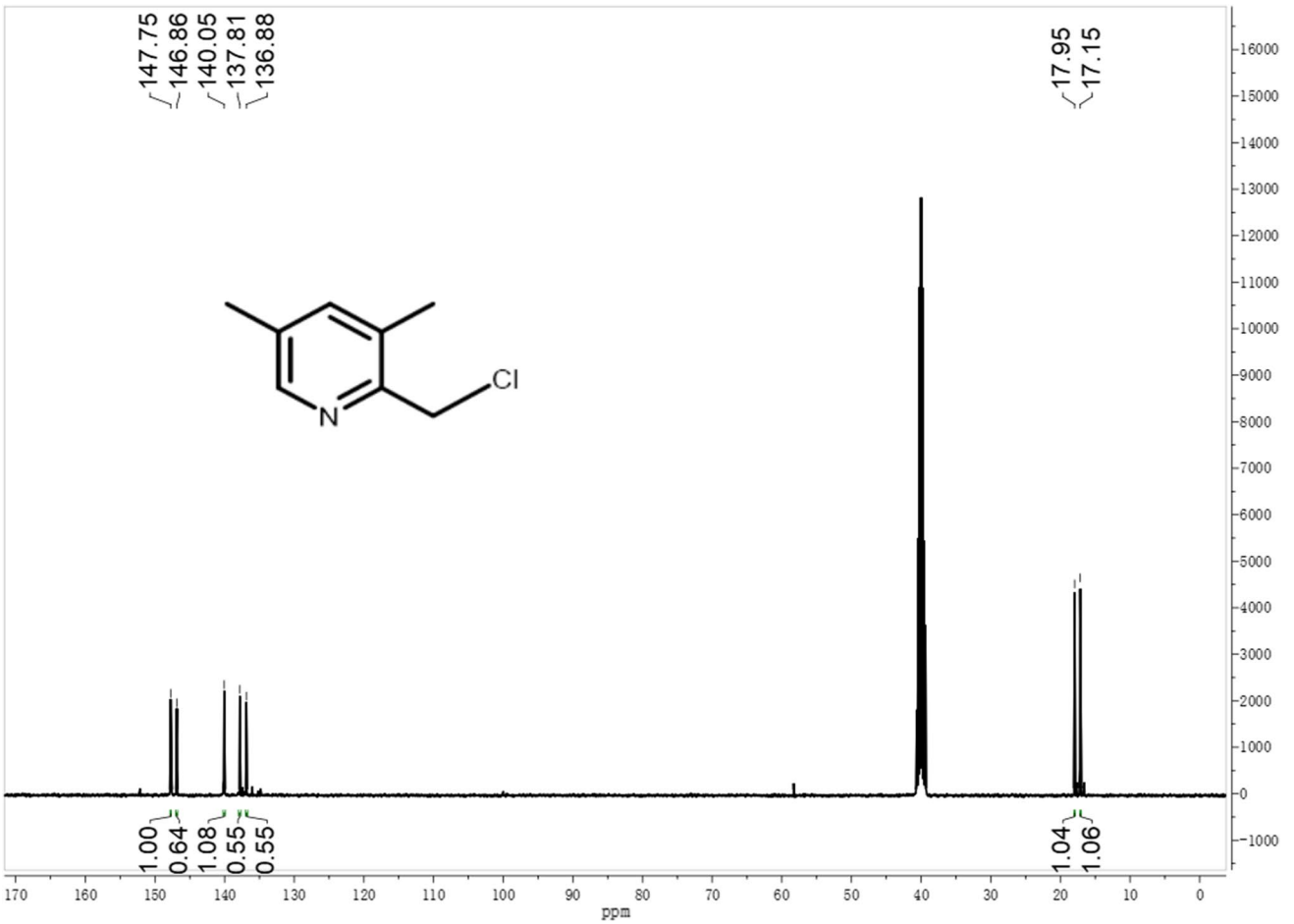

Fig. 8 ^{13}C NMR of compound **4**

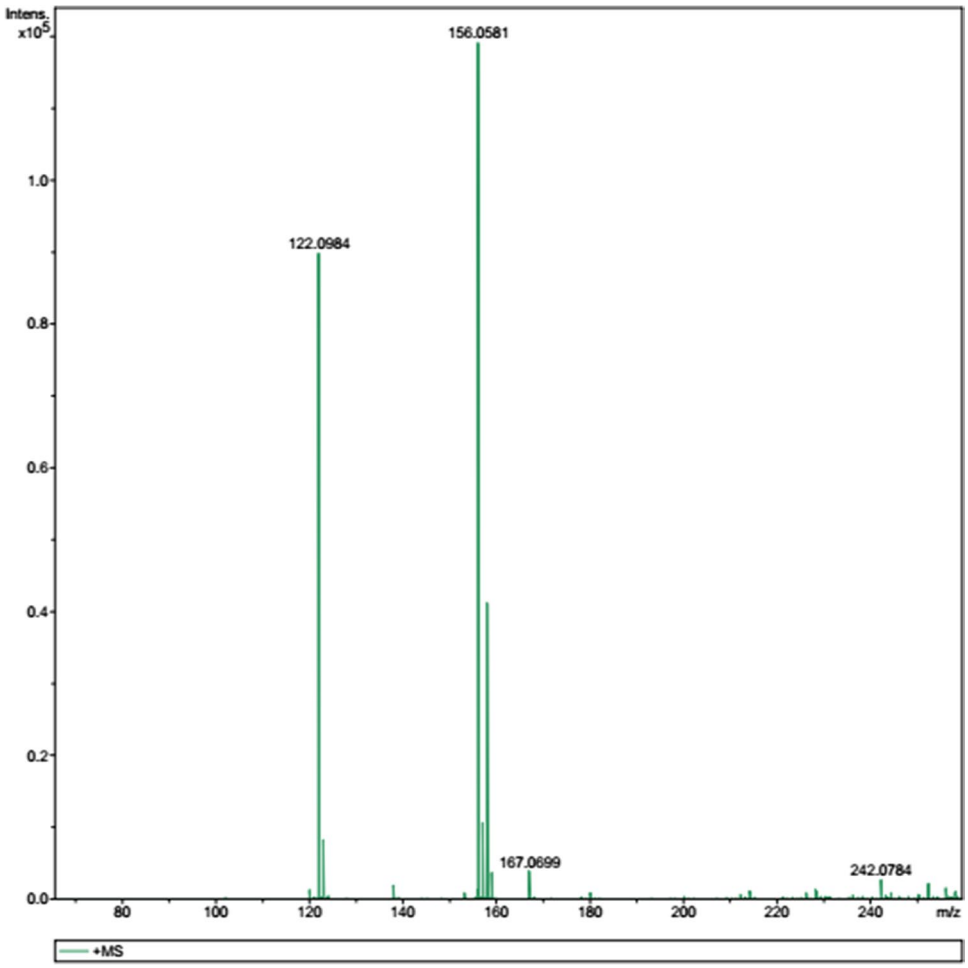

Fig. 9 Mass spectrometry of compound **4**

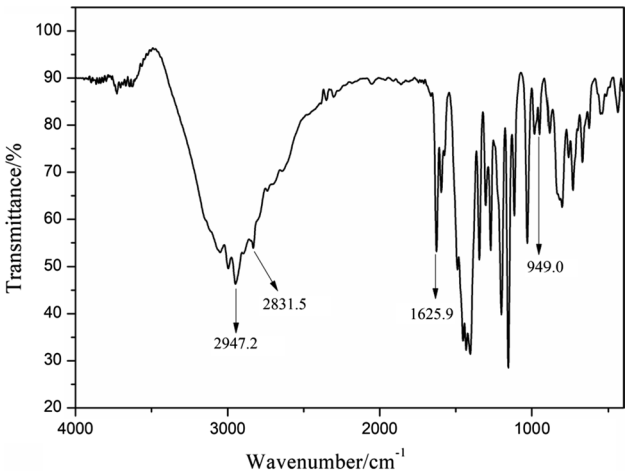

Fig. 10 FT-IR of compound **5**

In their work, the preparation of compound **2** is as follows: To a stirred solution of commercially available 2,3,5-collidine, AcOH and 30% aq. H_2O_2 solution were added. The mixture was heated at 80℃ for 6 h. In their work, compound **2** was prepared by adding hydrogen peroxide at one time, and the yield was 57%. In this paper, the method of dropping hydrogen peroxide can not only shorten the reaction time, but also increase the yield. The yield can reach 92.1%. Next, compound **2** reacted with acetic anhydride and needed to be purified by using silica gel column before the next reaction could take place. In this paper, compound **2** can be further reacted without purification. This simplifies the operation process and saves time.

The preparation of compounds **4**, **5** and **1** has not been reported in the literature. In this paper, the target products can be prepared by simple experimental methods, and the repeatability of the experiment has been guaranteed. The general process of the experiment is as follows:

During the preparation, 2, 3, 5-trimethylpyridine was first oxidized to give 2,3,5-trimethylpyridine-*N*-oxide (compound **2**) by H_2O_2 in acetic acid solution. Then compound **2** was reacted with acetic anhydride to obtain 3,5-dimethyl-2-hydroxymethylpyridine (compound **3**) via rearrangement and hydrolysis, which was further converted to the key intermediate 2-chloromethyl-3, 5-dimethylpyridine hydrochloride (compound **4**) by reacting with thionyl chloride.

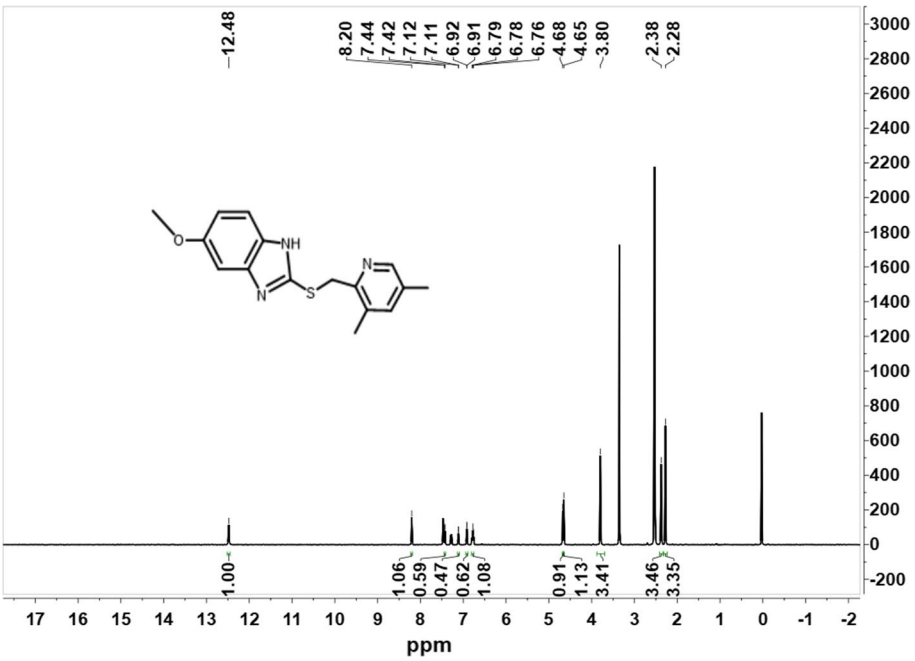

Fig. 11 ^{1}H NMR of compound **5**

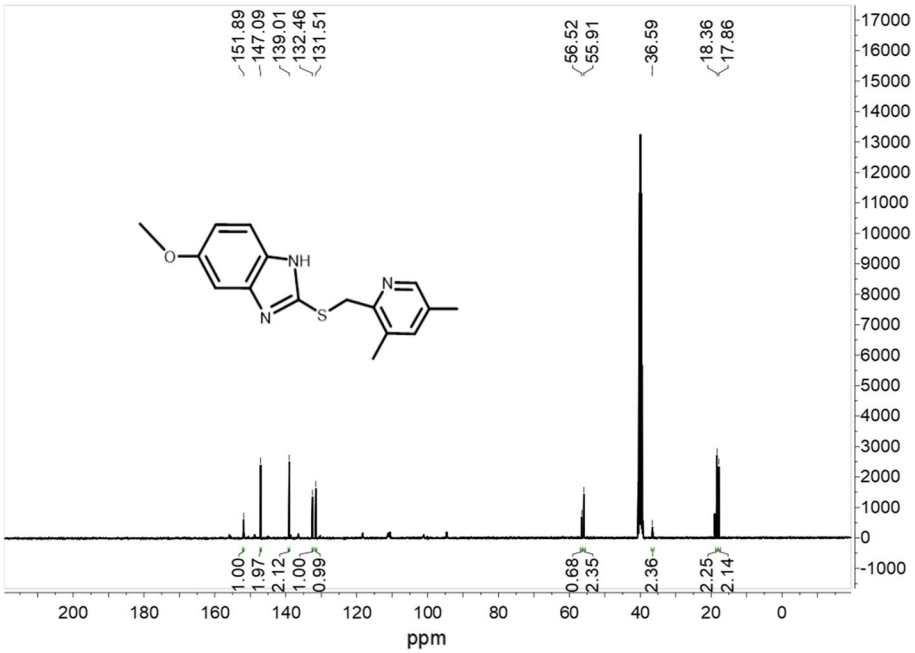

Fig. 12 ^{13}C NMR of compound **5**

The reaction of compound **4** with 2-mercapto-5-methoxy-1*H*-benzimidazole via nucleophilic substitution in the presence of methanol formed 2-[(3, 5-dimethyl-2-pyridinyl) methylthio)]-5-methoxy-1*H*-benzimidazole (compound **5**). Finally, rel-2-[[(3,5-dimethyl-2-pyridinyl)methyl]sulfinyl]-6-methoxy-1*H*-benzimidazole (compound **1**) was obtained by the oxidation of compound **5** with m-chloroperbenzoic acid.

The data of compounds **2**, **3** detected by NMR and FTIR are consistent with the data reported in the literature, which indicates that compounds **2**, **3** have been prepared. At the same time, compounds **4**, **5**, **1** which did not have relevant data in the literature were detected by nuclear magnetic resonance, Fourier infrared analysis and high-resolution mass spectrometry. Through the analysis of the data, it is confirmed that the related compounds have been prepared.

Characterization data of compound **2**: compound **2** was characterized by FT-IR; the FT-IR spectroscopy shows C–H stretching vibration peaks at 3049.4 cm^{-1}, methyl peak at 2962.6 cm^{-1}, aromatic ring stretching vibration peaks

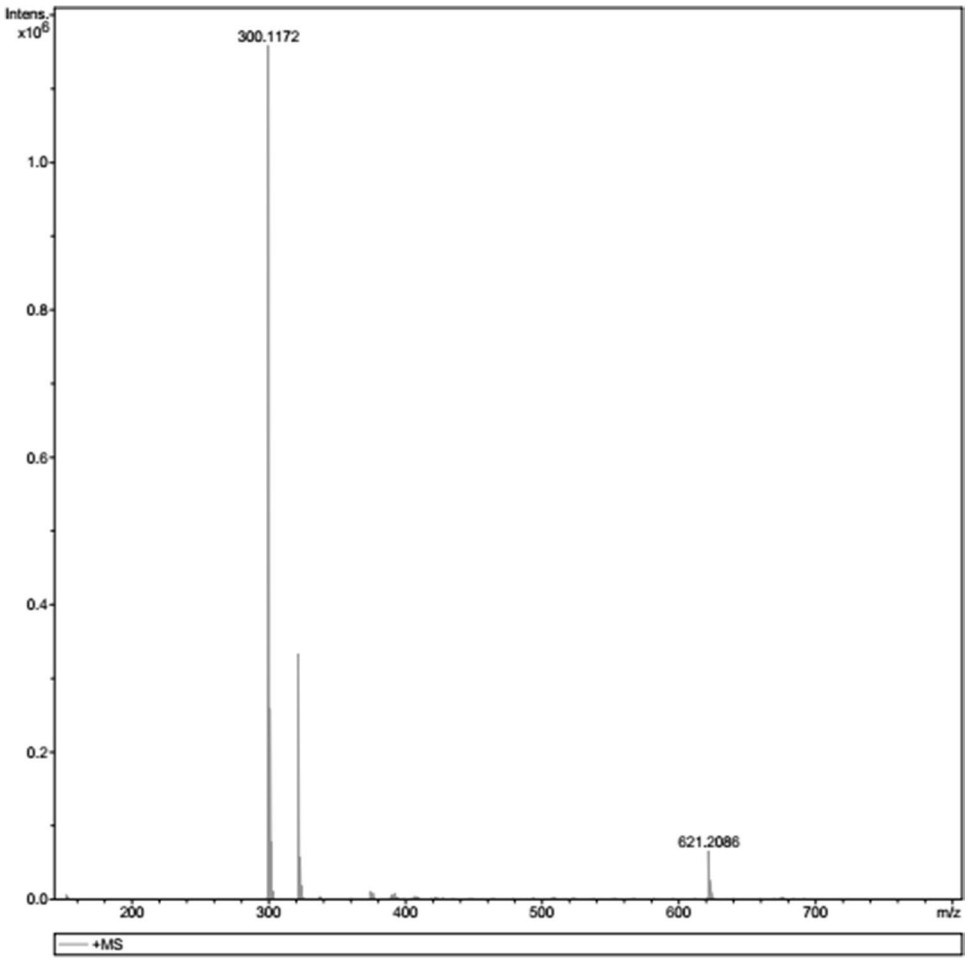

Fig. 13 Mass spectrometry of compound **5**

(skeleton bands) at 1577.7 cm^{-1} and out-of-plane bending vibration peaks of aromatic hydrogen at 756.1 cm^{-1} (Fig. 2). The ^{1}H NMR displayed nine protons at δ 2.23, 2.29 and 2.47 ppm corresponding to three methyl groups; δ 6.88 and 8.02 ppm corresponding to two tertiary hydrogen groups (Fig. 3).

Characterization data of compound **3**: the FT-IR spectroscopy shows that C–H stretching vibration peaks at 3000.9 cm^{-1}, aromatic ring stretching vibration peaks (skeleton bands) at 1573.9 cm^{-1}, out-of-plane bending vibration peaks of aromatic hydrogen at 777.3 cm^{-1} and O–H peaks at 3394.7 cm^{-1} (Fig. 3). The ^{1}H NMR displayed 6 protons at δ 2.18 and 2.31 ppm corresponding to two methyl groups; δ 7.29 and 8.22 ppm corresponding to two tertiary hydrogen groups; δ 4.65 ppm corresponding to one methylene group; δ 8.22 ppm corresponding to one methylene group (Fig. 7).

Characterization data of compound **4**: compound **4** was characterized by FT-IR, the FT-IR spectroscopy shows that the absorption peak of $–CH_2Cl$ can be seen at 675.1 cm^{-1}. At the same time, there are C–H stretching vibration peaks at 3024.8 cm^{-1}, aromatic ring stretching vibration peaks (skeleton bands) at 1562.4 cm^{-1} and out-of-plane bending vibration peaks of aromatic hydrogen at 773.0 cm^{-1} (Fig. 6). The ^{1}H NMR displayed six protons at δ 2.55 and 2.62 ppm corresponding to two methyl groups; δ 8.02 and 8.40 ppm corresponding to two tertiary hydrogen groups; δ 5.15 ppm corresponding to methylene (Fig. 7). In the ^{13}C NMR, the peak at 136.88–147.75 ppm is the carbon atom on the pyridine ring, and the peaks at 17.15 and 19.95 ppm are two primary carbons (Fig. 8). It can be seen from the high-resolution spectra that the molecule with mass fraction of 156.0581 is consistent with the theoretical calculation of compound **4**. The theoretical value of compound **4** $[M+H]^{+}$ is 156.0580 (Fig. 9).

Characterization data of compound **5**: FT-IR spectroscopy show that the absorption peak of –S– can be seen at 949.0 cm^{-1}, C–H stretching vibration peaks at 3049.5 cm^{-1}, aromatic ring stretching vibration peaks (skeleton bands) at 1489.0 cm^{-1}, out-of-plane bending vibration peaks of aromatic hydrogen at 761.9 cm^{-1}, and methyl peak at 2947.2 cm^{-1} (Fig. 10). The ^{1}H NMR displayed 6 protons at δ 2.28 and 2.38 ppm corresponding to two methyl groups, δ 3.80 ppm corresponding to a methoxy group, δ 12.48 ppm corresponding to N–H (Fig. 11). In the ^{13}C NMR, the

Fig. 14 FT-IR of compound **1**

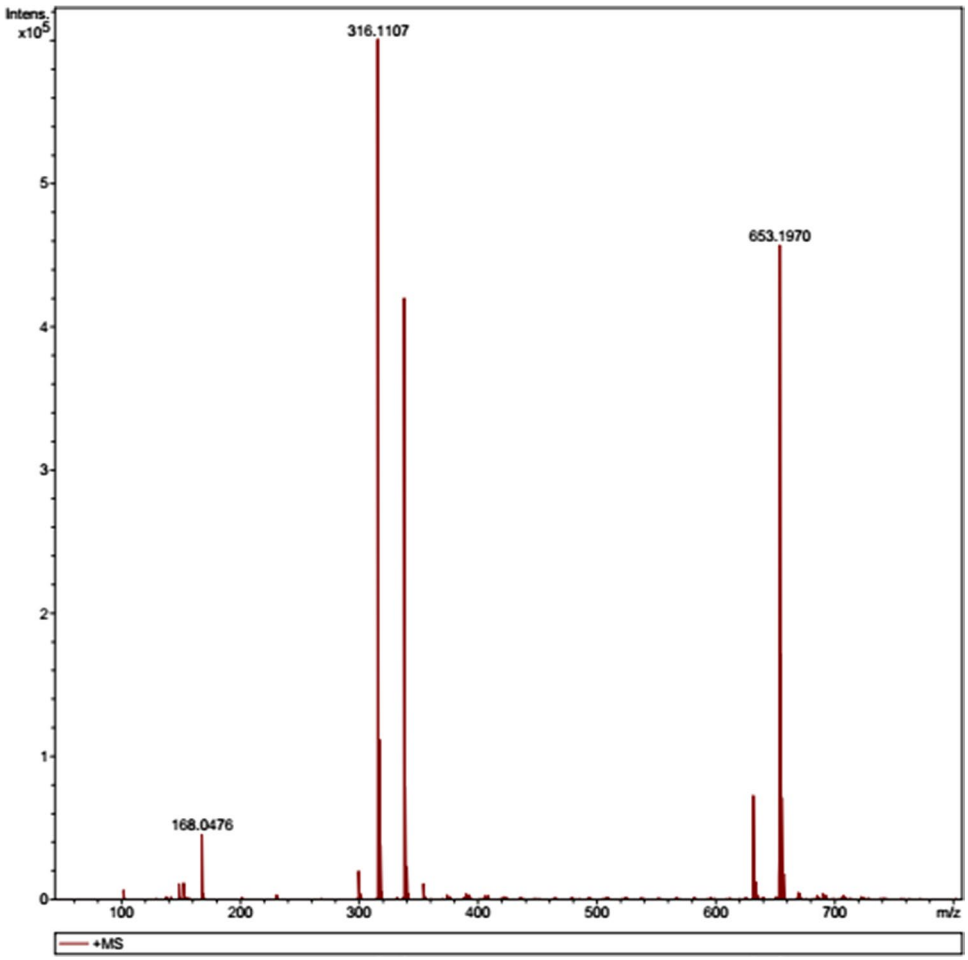

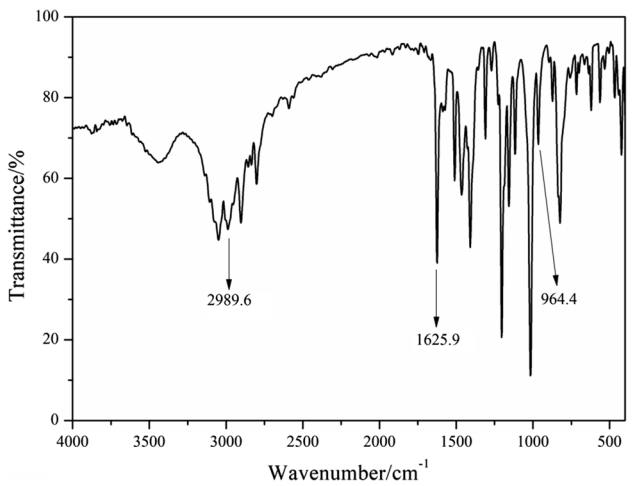

Fig. 15 ^{1}H NMR of compound **1**

number of carbon atoms in the test results is consistent with the target product (Fig. 12). It can be seen from the high-resolution spectra that the molecule with mass fraction of 300.1172 is consistent with the theoretical calculation of compound **5**. The theoretical value of compound **4** $[M+H]^+$ is 300.1171 (Fig. 13).

Characterization data of compound **1**: compound **1** was characterized by FT-IR; the FT-IR spectroscopy shows that C–H stretching vibration peaks at 3049.5 cm^{-1}, methyl peak at 2989.6 cm^{-1}, aromatic ring stretching vibration peaks (skeleton bands) at 1510.3 cm^{-1} and out-of-plane bending vibration peaks of aromatic hydrogen at 715.6 cm^{-1}. A sharp band could be observed at 964.4 cm^{-1} in the infrared spectra, which was attributed to S=O stretching (Fig. 15). The proton NMR spectra displayed six protons at δ 2.25 and 2.28 ppm corresponding to two methyl groups, δ 3.81 ppm corresponding to a methoxy group, δ 13.45 ppm corresponding to N–H, and δ 4.65 ~ 4.77 ppm corresponding to methylene (Fig. 16). In the ^{13}C NMR, the number of carbon atoms in the test results is consistent with the target product (Fig. 17). It can be seen from the high-resolution spectra that the molecule with mass fraction of 316.1107 is consistent with the theoretical calculation of compound **5**. The theoretical value of compound **4** $[M+H]^+$ is 316.1120 (Fig. 14). Based on the characterization data, it is possible to determine that the target product has been synthesized. In

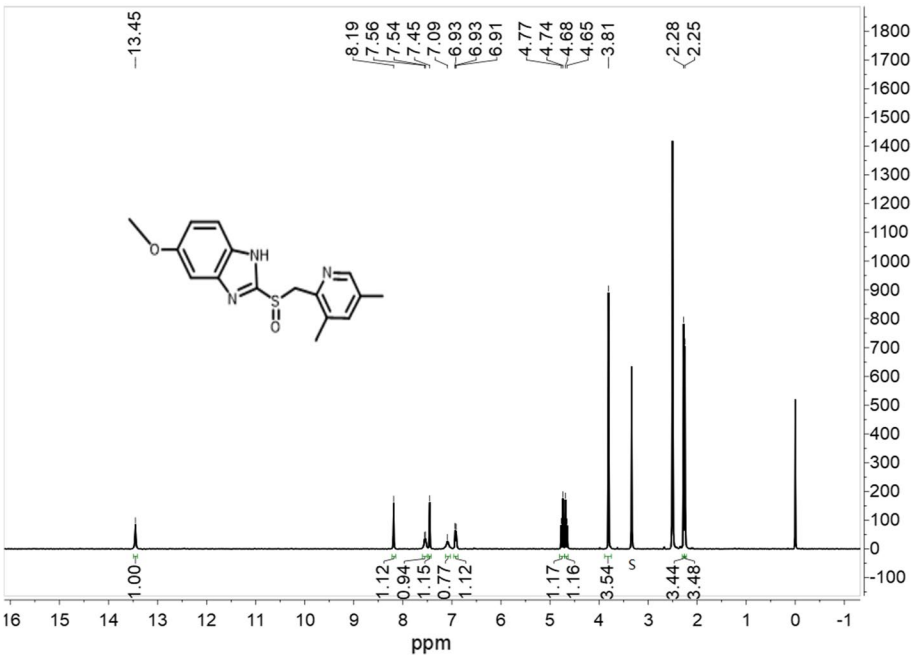

Fig. 16 ^{13}C NMR of compound **1**

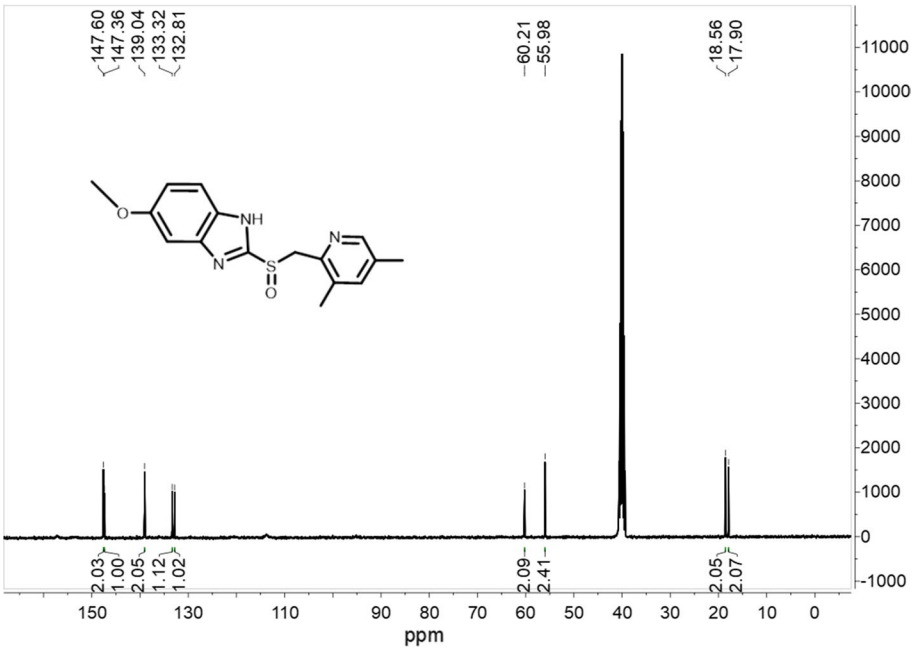

Fig. 17 Mass spectrometry of compound **1**

this synthetic method, the purity of the target product was as high as 99.58% (Fig. 18, Table 1).

Conclusion

A simple novel method to synthesize an impurity in esomeprazole has been developed. All raw materials used in the synthetic process were of low cost and easily obtained. Furthermore, from raw materials to compound **5**, all intermediate products did not have to be chromatographed, which could be directly used as the raw material for the next step. Thus, the reaction time was greatly reduced, and the production efficiency was greatly improved. Meanwhile, the synthetic method has the advantages of readily available raw materials, simple operation and mild reaction. Most important of all, the purity of the target product obtained by this synthetic route is high enough to supply kinds of research for detection and control of esomeprazole impurities.

Fig. 18 HPLC of compound **1**

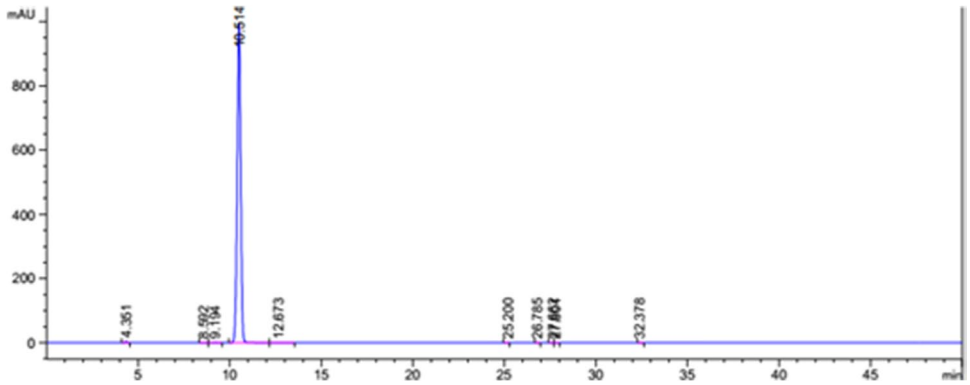

Table 1 Data analysis of HPLC

Peak#	Retention time [min]	Type	Peak width [min]	Peak area [mAU*s]	Peak height [mAU]	Peak area %
4	10.514	BB	0.2072	1.32697e4	997.70233	99.5839

Acknowledgements This work is supported by Natural Science Foundation of Shandong Province (ZR2016EMM13), Natural Science Foundation of Shandong Province (ZR2017LC005) and the Key Research and Development Program of Shandong Province of China (Major Science and Technology Innovation Project) (2018 CXGC1107).

References

And Ellervik U, Magnusson G (2010) A high yielding chemical synthesis of sialyl Lewis x tetrasaccharide and Lewis x trisaccharide; examples of regio- and stereodifferentiated glycosylations. J Org Chem. https://doi.org/10.1002/chin.199921210

Andersson T, Röhss K, Bredberg E, Hassan-Alin M (2001) Pharmacokinetics and pharmacodynamics of esomeprazole, the *S*-isomer of omeprazole. Clin Pharmacokinet 15:1563–1569. https://doi.org/10.1046/j.jcis1365-2036.2001.01087.x

Boekelheide VC, Linn WJ (1954) Rearrangements of *N*-oxides. a novel synthesis of pyridyl carbinols and aldehydes. J Am Chem Soc 76:1286–1291. https://doi.org/10.1021/ja01634a026

Cardile S, Romano C (2012) Clinical utility of esomeprazole for treatment of gastroesophageal reflux disease in pediatric and adolescent patients. Adolesc Health Med Ther 3:27–31. https://doi.org/10.2147/ahmy.s23193

Cheng HC, Wu CT, Chang WL, Cheng WC, Chen WY, Sheu BS (2014) Double oral esomeprazole after a 3-day intravenous esomeprazole infusion reduces recurrent peptic ulcer bleeding in high-risk patients: a randomised controlled study. Gut 63:1864–1872. https://doi.org/10.1136/gutjnl-2013-306531

Getter T, Zaks I, Barhum Y, Ben-Zur T, Böselt S, Gregoire S, Viskind O, Shani T, Gottlied H, Green O, Shubely M, Senderowitz H, Israelson A, Kwon I, Petri S, Offen D, Gruzman A (2015) A chemical chaperone-based drug candidate is effective in a mouse model of amyotrophic lateral sclerosis (ALS). ChemMedChem 10:850–861. https://doi.org/10.1002/cmdc.201500045

Manimaran T, Stahly GP (1993) Optical purification of profen drugs. Tetrahedron Asymmetry 4:1949–1954. https://doi.org/10.1016/s0957-4166(00)80436-x

Reddy PS (2013) Complexity in estimation of esomeprazole and its related impurities' stability in various stress conditions in low-dose aspirin and esomeprazole magnesium capsules. Sci Pharm 81:475–492. https://doi.org/10.3797/scipharm.1212-13

Stawny M, Piekarski M, Marciniec B (2016) Analysis of drug impurities. Handbook of trace analysis. Springer, Cham. https://doi.org/10.1007/978-3-319-19614-5_8

Sugano K, Kinoshita Y, Miwa H, Takeuchi T (2012) Randomised clinical trial: esomeprazole for the prevention of nonsteroidal anti-inflammatory drug-related peptic ulcers in Japanese patients. Aliment Pharmacol Ther 36:115–125. https://doi.org/10.1111/j.jcis1365-2036.2012.05133.x

Sugimoto M, Furuta T (2012) Efficacy of esomeprazole in treating acid-related diseases in Japanese populations. Clin Exp Gastroenterol 5:49–59. https://doi.org/10.2147/ceg.s23926

Tang RS, Wu JC (2013) Managing peptic ulcer and gastroesophageal reflux disease in elderly Chinese patients—focus on esomeprazole. Clin Interv Aging 8:1433–1443. https://doi.org/10.2147/cia.s41350

Thitiphuree S, Talley NJ (2000) Esomeprazole, a new proton pump inhibitor: pharmacological characteristics and clinical efficacy. Int J Clin Pract 54:537. https://doi.org/10.2169/internalmedicine.39.864

Tonini M, Vigneri S, Savarino V, Scarpignato C (2001) Clinical pharmacology and safety profile of esomeprazole, the first enantiomerically pure proton pump inhibitor. Dig Liver Dis 33:600–606. https://doi.org/10.1016/s1590-8658(01)80115-8

Vakil NB, Shaker R, Johnson DA, Kovacs T, Baerg RD, Hwang CEA, D'Amico D, Hamelin B (2001) The new proton pump inhibitor esomeprazole is effective as a maintenance therapy in GERD patients with healed erosive oesophagitis: a 6-month, randomized, double-blind, placebo-controlled study of efficacy and safety. Aliment Pharmacol Ther 15:927–935. https://doi.org/10.1046/j.jcis1365-2036.2001.01024.x